energies

MDPI

Article

Impact of Uninsulated Slab-on-Grade and Masonry Walls on Residential Building Overheating

Tadeusz Kuczyński [1] and Anna Staszczuk [2,*]

[1] Institute of Environmental Engineering, University of Zielona Góra, Prof. Z. Szafrana Str. 15, 65-516 Zielona Góra, Poland; t.kuczynski@iis.uz.zgora.pl
[2] Institute of Civil Engineering, University of Zielona Góra, Prof. Z. Szafrana Str. 1, 65-516 Zielona Góra, Poland
* Correspondence: a.staszczuk@ib.uz.zgora.pl

Abstract: Studies of the effects of removing underfloor insulation and increasing the thermal capacity of building walls are currently found almost exclusively in existing vernacular architecture and rammed-earth buildings, mostly in countries with warm climates. This paper proposes the combined use of these two measures to reduce the risk of overheating in a detached single-family house in a temperate climate during the summer. Experimental studies conducted during the largest heat wave on record in the summer of 2019 showed that peak daytime temperatures decreased by 5.2 °C to 7.1 °C, and peak nighttime temperatures decreased by 4.7 °C to 6.8 °C. Simulation studies taking into account occupant heat showed that the proposed passive methods could, under the IPCC 8.5 scenario, eliminate the need for mechanical cooling in a detached single-family house in the temperate climate of Central and Eastern Europe by 2100. The actual heating energy consumption for the building with an uninsulated floor and increased wall heat capacity was 5.5 kWh/m^2 higher than for the reference building, indicating that it can be a near-zero energy building. The proposed concept is in line with the new approach to the energy design of buildings, which should not be limited to reducing thermal energy demand, but should also respond to the needs arising from global warming.

Keywords: temperate climate; heat waves; building overheating; floor ground coupling

Citation: Kuczyński, T.; Staszczuk, A. Impact of Uninsulated Slab-on-Grade and Masonry Walls on Residential Building Overheating. *Energies* **2023**, *16*, 7558. https://doi.org/10.3390/en16227558

Academic Editor: Fabio Polonara

Received: 23 October 2023
Revised: 7 November 2023
Accepted: 10 November 2023
Published: 13 November 2023

1. Introduction

1.1. The Impact of Global Warming on External and Internal Temperatures and Human Health

Over the past few years, the intensity, frequency, and duration of heat waves have increased in temperate countries [1,2], with the period 2013–2022 experiencing the 11 hottest years on record [3]. The most intense heat waves in temperate European countries occurred in 2018 [4,5] and 2019 [6,7]. During the summer of 2019, most temperate European countries experienced exceptionally severe heat waves with many consecutive days with temperatures above or just below 30 degrees Celsius. France, Germany, Belgium, and the Netherlands, among others, had the warmest summers ever in the history of measurements [6]. Outdoor temperatures during the June heatwave in the mid-western regions of Poland reached levels higher than those predicted for the end of the 21st century assuming the worst-case IPCC8.5—hot scenario. At Zielona Gora, Poland, the average temperature for June 2019 was 22.7 °C, which is 6.2 °C above the long-term average for this month and 3.7 °C above the long-term average for July, the warmest month of the year. The average daily maximum temperature for the same period was 30.1 °C, which is 7.9 °C above the multi-year average [7]. The extreme heat waves expected in the next decades of the 21st century, coupled with possible power outages, are likely to have a negative impact on the health and comfort of residents [8] and lead to increased morbidity and mortality [9], with the majority of heat-related deaths occurring in buildings in developed countries [10]. During the 2019 summer heat wave, more than 2500 deaths were reported across Europe [11]. The highest number of deaths was 1435 in France [12], 900 in the United Kingdom [13], 716 in Belgium [14], and 500 in Germany [15].

1.2. Passive Measures against Building Overheating

The experience of developed countries with temperate climates shows that the most common response to prolonged periods of severe heat waves is the installation of mechanical cooling systems [16,17]. However, the heat dissipated by mechanical air conditioning systems, together with the heat removed by air exchange, is the main source of anthropogenic heat, leading to rising temperatures, especially at night [18], and a shift of peak electricity demand to late evening and night. This can lead not only to increased demand for electricity at these times but also to a reduction in the viability of increasingly common solar-based renewable energy systems, which are not available at these times [19].

Passive cooling measures could significantly reduce the demand for space cooling [20,21]. These include measures to reduce solar gain (e.g., shading), to remove internal heat (e.g., night ventilation), or to modulate the heat transfer profile (e.g., high thermal inertia) [21]. The two main passive measures of preventing overheating in summer: night ventilation and window shading are highly dependent on occupant behavior [22,23].

While the effectiveness of night ventilation or window shading is directly related to occupant values, expectations, and therefore behavior, the thermal capacity of a building is a feature of the building that is independent of the occupants' behavior. Newly designed buildings can effectively use traditional high thermal mass materials to mitigate overheating [24–28].

1.3. Defining of Research Goal

In 2015, the effect of replacing lightweight frame walls with cellular concrete walls was studied in detached single-family experimental buildings in Nowy Kisielin. During the same period, the effect of the removal of floor insulation in two south-facing rooms of 6.0 m × 3.0 m × 3.4 m was compared in another experimental building in Nowy Kisielin. The results of the study were published in Kuczyński and Staszczuk [29] and Staszczuk et al. [30], respectively. Replacing the lightweight frame walls with cellular concrete block walls reduced the average maximum indoor air temperature during the heat wave by 2.8 °C. Removing the floor insulation in the high thermal capacity room reduced the maximum temperature by almost 4 °C. The results of the individual passive strategies presented in this study do not necessarily add up, especially as they were tested in different buildings with different locations, dimensions, window-to-floor ratios, etc.

The research goal was to determine the combined effect of the use of two passive strategies, independent of occupant habits and behavior, in a single-family detached house in a temperate climate. Given their individual effectiveness, it was expected that their combined effect would lead to a significant reduction in the number of hours during which the internal temperature exceeds the permitted values, and also to a significant reduction in the energy required for cooling.

Since the removal of thermal insulation from the floor of the building leads to an increase in heat demand during the heating season, and the magnitude of this increase may determine the suitability of the proposed solutions, it was necessary to determine the magnitude of this increase. For this purpose, the authors determined theoretically and experimentally the heat demand of the building during the winter of 2019/2020.

In order to allow for a more complete interpretation of the experimental results obtained, the temperature of the soil beneath the floor was monitored and recorded for the entire period of the study.

1.4. Novelty of the Work

In view of the current energy policy, which in countries with a temperate climate is aimed at reducing the demand for heating energy during the heating season, few studies have addressed the potential benefits for thermal comfort of using an uninsulated floor on the ground during hot summer days. This paper is the first attempt, to the authors' knowledge, to experimentally verify the effectiveness of the combined effect of these two passive solutions for increasing the thermal capacity of a building: replacing the lightweight

walls of a building with medium-weight ones and removing the thermal insulation of the ground floor in full-size energy-efficient detached residential buildings during the warmest summer ever recorded in Poland.

The aim of this article is to assess the impact on energy consumption and occupant thermal comfort of commonly used but discouraged passive methods, such as masonry walls, or even prohibited methods, such as uninsulated ground floors.

In addition to summer performance, the effect of the proposed solutions on energy demand during the heating period was also analyzed in order to illustrate the full impact of the proposed solutions.

The proposed passive cooling methods are not new but come out of the tradition of vernacular architecture. Moreover, in many EU countries, single-family dwellings with walls of high thermal capacity building materials, with the floor on the ground without thermal insulation, still account for a significant share of the current housing stock in operation. In 2018, approximately 2% of the housing stock in operation in Poland was built using lightweight frame construction. In subsequent years, the share of these structures did not exceed 1–1.5% of all residential buildings constructed [31]. Standards requiring the use of horizontal insulation of the floor on the ground emerged in Poland in the last 20 years. During this period, no more than 25% of current residential buildings were built. At the same time, the increase in temperatures as a result of global warming, especially in temperate countries, is leading to increasingly mild winters and hot summers and, as a result, an interest not only in the energy needed for heating but also in that required for cooling.

The authors hypothesize that with good insulation of the roof, external walls, and windows of a building, in combination with the use of mechanical ventilation with heat recovery, such a building can meet the criteria of a near-zero energy building.

2. Methodology

2.1. Experimental Investigation

2.1.1. Characteristics of Experimental Buildings

The research was carried out in two real-scale objects, located in The Science and Technology Park of the University of Zielona Góra in Nowy Kisielin—a small district in the city of Zielona Góra in Poland (Cfb-climate according to [32]). Experimental buildings were designed to be almost identical except for the construction of their external and internal walls; building B1 (on the left in Figure 1)—traditional masonry construction and building B2 (on the right in Figure 1)—lightweight skeletal timber framed walls both external and internal.

Figure 1. Experimental buildings.

External walls in traditional buildings were made of cellular concrete blocks—24 cm and insulated with 20 cm of mineral wool. The internal walls, both structural and partitioning, were made of 24 cm and 8 cm thick sand-lime (silicate) blocks. The external walls of the

skeleton building are made of a timber frame filled with 16 cm of mineral wool, additionally insulated with 18 cm of mineral wool. The internal walls both construction and partitioning were made of wood frame filled with 16 cm and 5 cm of mineral wool, respectively. Details of their structural solutions and materials, as well as the main dimensions of the buildings and individual rooms, are presented in the study by Kuczynski and Staszczuk [29]. The living area of the laboratory buildings is similar (122 m^2). They have the same orientation of the main façade and the same arrangement of the rooms (Figure 2, Section 2.1.2). The research is conducted in unoccupied buildings to eliminate the influence of different user preferences and behaviors on the measurement results [25,33].

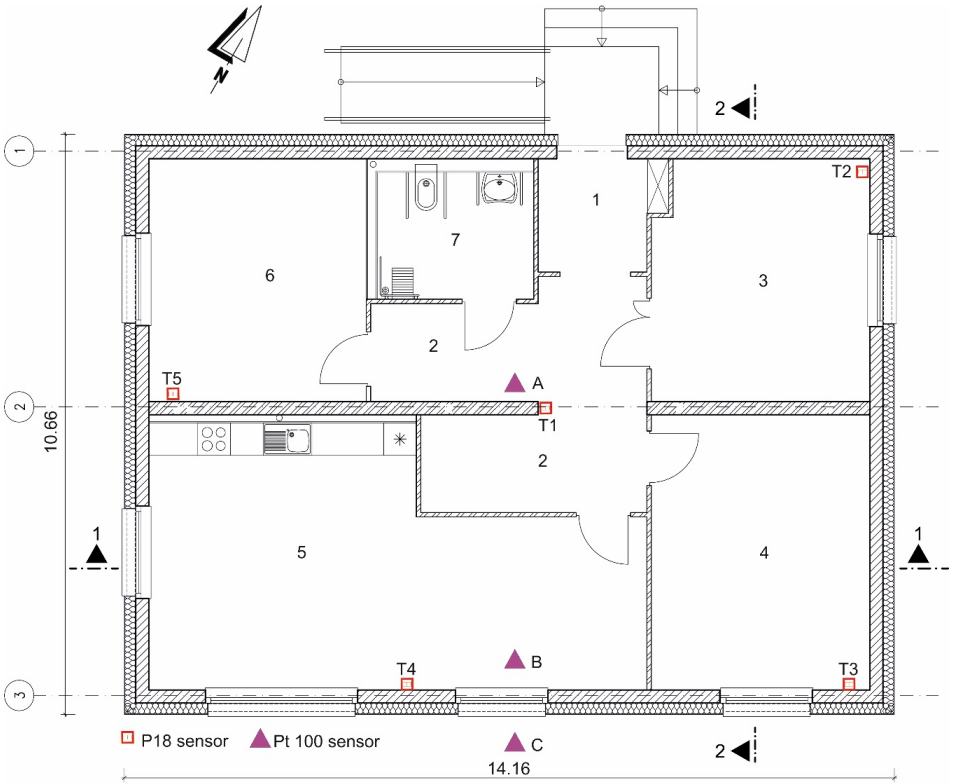

Figure 2. Plan of the building B1 with location of sensors; 1—vestibule, 2—hall, 3—bedroom, 4—bedroom, 5—living room with kitchen annex, 6—bedroom, 7—bathroom; T_1, T_2, T_3, T_4, T_5—sensors to measure of indoor air temperature; A, B, C—sensors to measure of ground temperature.

In 2019, in building B1 with increased thermal capacity, a 30 cm layer of slab-on-grade thermal insulation was removed and replaced with concrete. The foundation wall was thermally insulated with 20 cm of EPS to a depth of 80 cm below ground level. Thermal properties of experimental building including new construction of slab-on-grade were presented in Table 1.

Table 1. Thermal properties of building partitions.

Assembly	B1			B2		
	U [W/m² K]	κ_m [kJ/m² K]	A [m²]	U [W/m² K]	κ_m [kJ/m² K]	A [m²]
External wall	0.138	97.00	116	0.126	37.33	116
Internal wall 1—construction wall	1.386	416.00	34	0.412	74.66	34
Internal wall 2—partition wall	1.987	160.00	62	0.829	45.00	62
Ceiling	0.086	11.25	122	0.106	17.30	123
Slab on ground	0.116	92.40	122	0.116	92.40	123
Slab on ground after modification	0.796	158.76	122			

Thermal heat capacity (κ_m) was calculated according to ISO 13,786 [34] and used to determine the TMP variable (Thermal Mass Parameter), that characterizes the thermal mass of the building according to the following formula [35]:

$$TMP = \frac{\sum \kappa_m \cdot A}{TFA} \quad (1)$$

where A is the surface area of all the internal building partitions and TFA is its total floor area.

The sum of the thermal capacity is understood to be the thermal capacity of all walls (both external and internal), as well as the floors and roofs enclosing the buildings. The TMP values are 400 kJ/m^2 K for the B1 building and 192 kJ/m^2 K for the B2 building. They classify these buildings as medium and lightweight construction, respectively. After the modification of the floor slab in building B1 in 2019, its TMP value is 467 kJ/m^2 K. The building is classified as a heavy-weight structure.

2.1.2. Measurements

Experimental research concerns the period of one year (1 May 2019–30 April 2020). During this time, air temperature and relative humidity inside the building; energy demand; and outdoor parameters such as air temperature, relative humidity, and global horizontal solar radiation were recorded continuously. Inside both buildings and outside, the temperature of the ground at the depth of 1.5 m below slab-on-grade level was measured in three locations A (in the center of the building), B (0.5 m from the external wall to the inside of the building), and C (0.5 m from external wall to the outside of the building) presented in Figure 2.

Technical specifications of measuring devices are presented in Table 2.

Table 2. Technical specification of measurement devices.

Measurement Device	Measurement Parameter	Measuring Range	Accuracy/Error
P18—temperature and humidity transmitter. The installation location is shown in Figure 2. Installed at a height of 1.2 m above the floor surface.	Temperature of indoor air Humidity of indoor air	−30 . . . −20 . . . 60 . . . 80 °C 0 . . . 100%	±0.5% ±2% dla RH = 10 . . . 90% ±3% dla RH otherwise
Delta OHM, type HD9008TRR	Temperature of outdoor air	−40 . . . +80 °C	±0.15 °C ± 0.1% measured value
Shielded Delta OHM, type HD9007A1	Relative humidity of outdoor air	0 . . . 100%	1.5% RH (0 . . . 90% RH) ±2.0% RH otherwise
Delta OHM, type LP PYRA 03	Global solar radiation	0÷2000 W/m^2	Sensitivity: 5–15 µV/W m^2 Annual stability: <	±2.5	% Nonlinearity: <	±2	% Directional error: <	±22	W/m^2
Temperature sensor T-107 Pt100 kl.1/10B Temp. 1000C	Soil temperature	−200 . . . +400 °C	±(0.3 + 0.005 × t)

The equipment for measuring outdoor climate parameters was located at a meteorological station on the roof of building B1.

Indoor air temperatures in laboratory buildings were measured in five measuring points (Figure 2) and then averaged per area. The weighted average temperature was calculated according to the methodology described by the authors in [29]. Measuring point

T_1 covers temperatures in rooms: 1, 2, and 7; T_2 in room 3; T_3 in room 4, T_4 in room 5; and T_5 in room 6.

An independent freely programmable PLC controller (Figure 3) was provided for each of the experimental buildings, which collects measurements from the building and from the meteorological station, as well as controlling the devices in the building and mediating the data exchange between the SCADA system (a computer system for the collection of current measurement data, their visualization, process control, alarming, and data archiving).

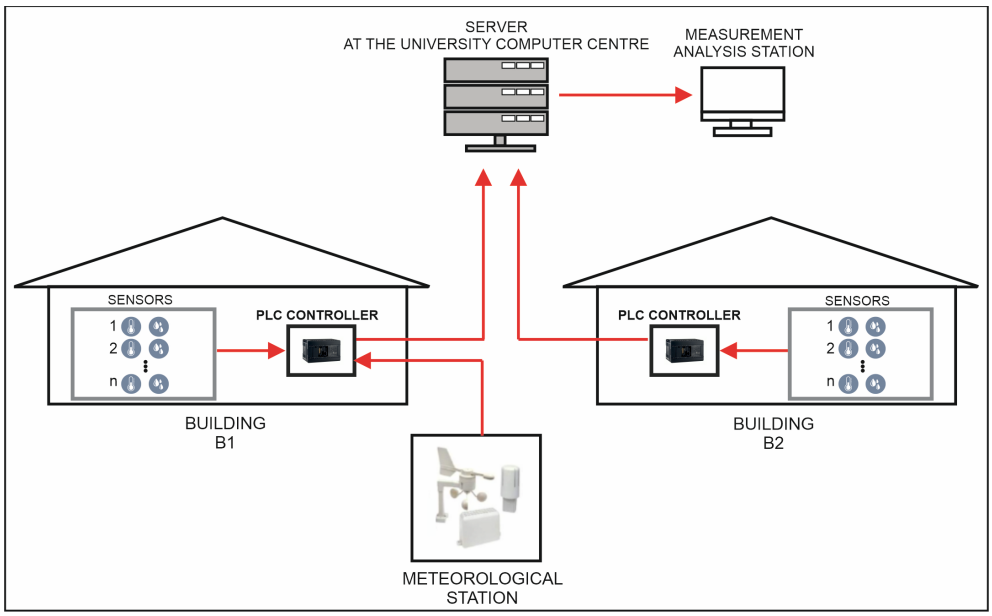

Figure 3. Schematic of the measurement system in research buildings B1 and B2.

For the study, a server located outside the buildings in the Computer Center was provided for the acquisition of measurement data from the buildings. An operator station was placed on the premises of the Science and Technology Park and the University of Zielona Góra to present and analyze historical data collected on the server, as well as to monitor and control both buildings. It was also possible to perform these activities online via a remote desktop.

Measurement results from the P18 sensors and from the meteorological station were recorded in the SCADA system with a frequency of every 5 min, and from the T-107 Pt100 sensors—every 0.5 min. Measurement results from the meteorological station, due to the dynamic nature of changes in the external climate parameters, were taken for analysis at 5 min intervals and then averaged to 1 h. Due to the slowly varying nature of the internal and in-ground parameters, experimental results in this study were taken at hourly intervals.

In all rooms, the air exchange rate was kept constant at 0.6 per hour. The rooms were supplied with air through inlet diffusers, which made it possible to adjust the amount of supply air to the volume of the rooms so that the air exchange in the rooms was the same. Passive measures such as night ventilation or the closing of external blinds, the effectiveness of which depends on user behavior (see Section 1), were not used. The buildings were mechanically ventilated, with heat recovery switched on during the heating period and circulation via an external bypass during periods when heating was not required.

Four 1 kW electric heaters and one 1.5 kW electric heater were used to heat each of the buildings. The set point of indoor air temperature was 20 °C and kept constant during the heating season.

2.2. Computer Simulations

2.2.1. Numerical Model

The experimental research was carried out in unoccupied buildings to eliminate the influence of different user preferences and behaviors on the measurement results. A numerical model of research buildings B1 and B2 was created (Figure 4) to take into account heat gains from occupants. Design Builder software v. 6.1.8.21 was used, which allowed the building geometry to be reproduced according to the architectural design. The parameters of the building materials were determined from the manufacturer's data and, in their absence, were taken from the software's database. The model was divided into 7 thermal zones, corresponding to the number of rooms used in the building.

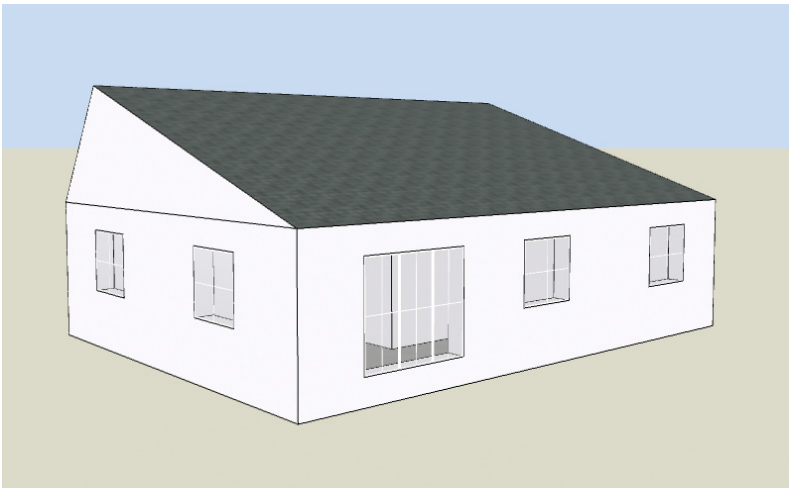

(**a**)

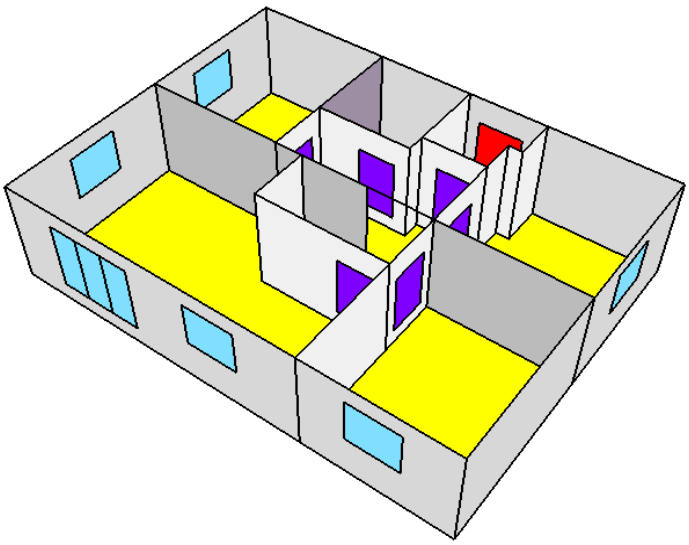

(**b**)

Figure 4. Computational model of laboratory buildings; (**a**)—visualization, (**b**)—cross-section.

Numerical simulations were carried out in the EnergyPlus software v. 9.6.0. The choice of EnergyPlus as the simulation engine was determined, among other things, by the high quality of the calculation results and the great flexibility in the construction of the model.

The weather data for the Nowy Kisielin location, including all parameters from the local meteorological station, was prepared in the '.epw' weather file format [36]. This is a typical file format commonly used in EnergyPlus, based on a CSV text file, which contains a summary of hourly weather variables from the whole year for the location.

The heat transfer process at the surface of the partitions is considered in the programme by adopting a simple natural convection algorithm. In this model, constant coefficients are used for different heat transfer configurations. For the calculations in this paper, heat transfer coefficients were used in accordance with PN-EN ISO 6946 [37].

For assemblies touching the ground, it is important to determine the corresponding ground temperatures. This is significant for the thermally uninsulated floor, which is in direct contact with the ground with a high thermal capacity. The thermal coupling of the building to the ground is possible in EnergyPlus based on the ground heat transfer calculation using Site:GroundDomain:Slab [38].

2.2.2. Model Calibration

When calibrating models for assessing the thermal and energy performance of buildings, the most common parameters dealt with are those related to the outdoor climate [39,40], with the location of the building, including the degree of sunlight and potential shading [40], building characteristics such as thermal insulation and air tightness [39,41] and its ventilation, air conditioning and heating systems [40,42,43] as well as the conditions of use of the buildings and the equipment and systems installed in it [42,44]. By means of trial and error, the model was calibrated by modifying the air exchange through ventilation according to the measurements of its inlet velocity through the diffusers in the rooms of the two buildings. Subsequent calibration steps resulted from the airtightness tests carried out on the buildings, which showed that the airtightness was higher for the lightweight building and included further modification of air exchange through potential leaks in the building envelope (+10% for building B1 and −10% for building B2) and modification of the averaged heat transfer coefficient for the external envelope of the solid building (+5%).

Statistical indicators such as root mean square error RMSE [°C] and root mean square coefficient of variation Cv(RMSE) [%] were used to model calibration. They were calculated according to the following formulas:

$$\mathrm{RMSE} = \sqrt{\sum_{i=1}^{Ni} \frac{(T_m - T_c)^2}{Ni}} \tag{2}$$

$$\mathrm{Cv(RMSE)} = \frac{\mathrm{RMSE}}{\frac{1}{Ni}\sum_{i=1}^{Ni} T_m} \cdot 100 \tag{3}$$

where:

T_m—temperature of internal air measured [°C],
T_c—temperature of internal air calculated [°C],
N—number of measurements.

Pearson's linear correlation coefficient (r) was also used.

3. Results

3.1. Indoor Temperatures

The summer of 2019 was the warmest on record for meteorological measurements in Poland. The average outdoor temperature for the period 1 June to 31 August was 20.9 °C. This was 3.9 °C above the multi-year average, roughly in line with the IPCC's Middle 6.0 scenario for 2100, which projects a global temperature increase of 3–4 °C by that year. The outside temperature exceeded 30 °C on 28 days, including 15 days with temperatures of 32 °C. The average solar radiation was 227.0 W/m^2. Figure 5 shows the hourly temperature profile in both buildings during the three warmest months from 1 June to 31 August.

The average temperature in building B1 was 22.4 °C. The average temperature difference between the buildings was 5.4 °C. Maximum temperatures in building B2 exceeded 30 °C on 33 days and 31 °C on 14 days. In building B1, the temperature exceeded 25 °C only three times during the three summer months, on the last three days of August.

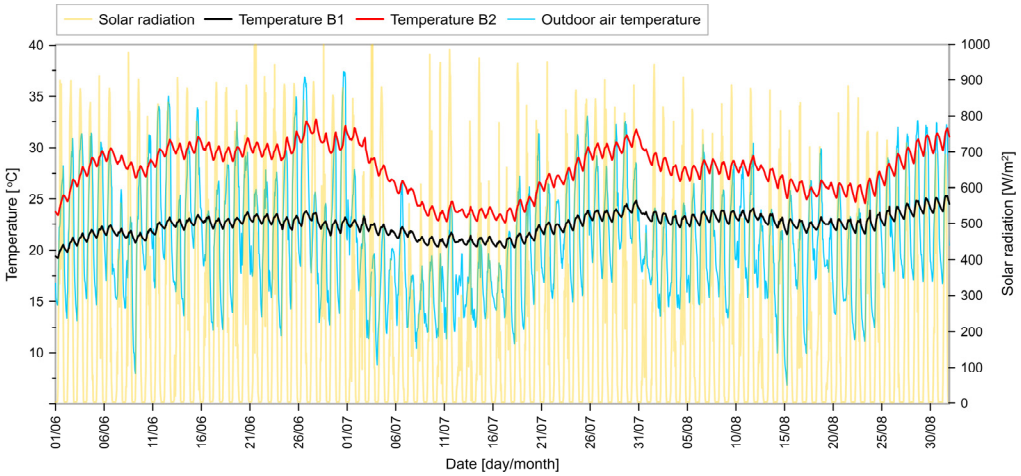

Figure 5. Hourly indoor temperatures in buildings B1 and B2 in June–August 2019.

In order to illustrate the impact of the applied passive strategies on the buildings' resilience to overheating during hot weather, the analysis should consider the whole summer period when excessive temperatures are expected, but also periods of heat waves when the outdoor temperature rises for a few days and then remains high for a few more days.

An analysis of the entire summer period is necessary as it allows the effectiveness of the adopted strategies to be assessed within the framework of generally applicable standards. An analysis of the effectiveness of the passive strategies adopted during heat waves, on the other hand, allows this to be done when this effectiveness is most needed. It should be emphasized that the effectiveness of passive strategies often depends on the climatic conditions, e.g., the high thermal capacity is particularly effective during periods of prolonged heat waves [7] and night ventilation is particularly effective during periods of high diurnal air temperature variations [45]. In temperate climates, there is rarely a need to use passive strategies during periods outside of heat waves. Therefore, conclusions about their effectiveness cannot be based only on average values of measurements over the whole summer period, but also on their values at extremely high temperatures.

Tables 3–5 summarize the average outdoor and indoor temperatures for buildings B1 and B2 and the average daytime and night-time peak temperatures for the three heat waves from 1 June to 31 August 2019. The average, maximum, and minimum outdoor temperatures during the June heatwave were 22.7 °C, 29.8 °C, and 14.9 °C, respectively, and were 6.0 °C, 8.7 °C, and 3.2 °C above the multi-year average for June (Table 3). Maximum temperatures exceeded 30 °C at sixteen days and 34 °C at six. Furthermore, the maximum outdoor temperature only fell below 25 °C twice. The days were especially hot, while the nights were not as oppressive.

Table 3. Average daily outdoor and indoor air temperatures in buildings B1 and B2 during the June 2019 heatwave.

Parameters Analyzed	T_o [°C]	T_i [°C]		
		B1	B2	B2 − B1
T_{min}	14.85	21.78	28.52	6.76
$T_{av.}$	22.69	22.34	29.25	6.91
T_{max}	29.83	22.86	30.00	7.14
$T_{max} - T_{min}$	14.97	1.09	1.46	
$(\Delta\theta_i/\Delta\theta_o)$		0.07	0.10	

Table 4. Average daily outdoor and indoor air temperatures in buildings B1 and B2 during the 18–30 July 2019 heatwave.

Parameters Analyzed	T_o [°C]	T_i [°C]		
		B1	B2	B2 − B1
T_{min}	16.34	22.00	26.91	4.91
$T_{av.}$	22.70	22.67	27.85	5.18
T_{max}	29.16	23.26	28.68	5.42
$T_{max} - T_{min}$	12.82	1.26	1.77	
$(\Delta\theta_i/\Delta\theta_o)$		0.10	0.14	

Table 5. Average daily outdoor and indoor air temperatures in buildings B1 and B2 during the heatwave from 22 August to 1 September 2019.

Parameters Analyzed	T_o [°C]	T_i [°C]		
		B1	B2	B2 − B1
T_{min}	15.54	22.85	27.53	4.68
$T_{av.}$	22.48	23.67	28.67	5.00
T_{max}	30.31	24.50	29.66	5.16
$T_{max} - T_{min}$	14.77	1.65	2.13	
$(\Delta\theta_i/\Delta\theta_o)$		0.11	0.14	

The average maximum temperature in building B2 exceeded 30 °C on 20 of the 30 days of the month and reached 31 °C on eight days. The average maximum temperature in building B1 only exceeded 24 °C twice. During the first week, the temperature in building B2 increased very rapidly and then remained at a similar level for the following days. The temperature changes in building B1 were notably less pronounced. At the beginning of the measurement period, the difference between the temperatures in the two buildings did not exceed 4.0 °C, reaching 8 °C on the hottest days of the month. The average difference between the maximum temperatures in both buildings was 7.1 °C and remained at a similar level both during the day and at night. The differences between the average maximum temperatures during the heatwave from 1 to 30 June 2019 for the bedroom and the living room were 7.2 °C and 7.0 °C, respectively.

After the June heat wave, the first half of July 2019 was much cooler. A new rise in outdoor temperatures began on 18 July and continued, with small interruptions, until 30 July. The values of the average outdoor temperature were the same as in the June wave and amounted to 22.7 °C. The average maximum temperature was slightly lower and the average minimum temperature slightly higher, 29.2 °C and 16.3 °C, respectively, with maximum outdoor temperatures exceeding 30 °C on five occasions (Table 4).

In the lightweight building (B2), the average indoor air temperature and the average maximum and minimum temperatures were 27.9 °C, 28.7 °C, and 26.9 °C, respectively. In building B1, where the floor insulation was removed, these temperatures were 22.7 °C, 23.3 °C, and 22.0 °C, respectively (Table 4).

The average maximum temperature in building B2 exceeded 30 °C on six of the 13 days of the heatwave and reached 31 °C on two days. The average maximum temperature in building B1 exceeded 24 °C three times. As in June, the temperature in building B2 rose much faster than in B1 during the first week. The average difference between the maximum temperatures in the two buildings was 5.4 °C, ranging from 3.3 °C to 6.9 °C and remaining at similar levels throughout the 24 h period.

The last heat wave of 2019 took place between 22 August and 1 September. The average outdoor temperature during this period was 22.5 °C, similar to the two previous waves in June and July. The average maximum and minimum outdoor temperatures were 30.3 °C and 15.5 °C, respectively (Table 5). During the 11-day heat wave, the maximum outdoor temperatures exceeded 31 °C for the last seven days.

In the lightweight building (B2), the mean indoor air temperature and the averaged maximum and minimum temperatures were 28.7 °C, 29.7 °C, and 27.5 °C, respectively, i.e., about 1 °C more than during the July heat wave (Table 5). In building B1, the values were 23.7 °C, 24.5 °C, and 22.9 °C, respectively, also about 1 °C more than during the previous heat wave. The average maximum temperature in building B2 exceeded 30 °C on six of the 11 days of the heat wave and 31 °C on four days. The average maximum temperature in building B1 exceeded 24 °C on eight days and 25 °C on four days. Throughout the heat wave, the temperature in building B2 increased faster than in B1. The average difference between the maximum temperatures in the two buildings was 5.2 °C, ranging from 3.3 °C to 6.6 °C.

3.2. Thermal Comfort Analysis

To better illustrate the extent to which the use of passive cooling strategies can affect the thermal comfort of occupants during high summer temperatures, national standards such as the American ASHRAE Standard 55 [46] or the English CIBSE TM52 [47] are often used in research papers. Both assume that measured or simulated values of indoor temperatures are related to the exponentially weighted running mean outdoor temperature (Trm), taking into account the adaptation of occupants to increasing high temperatures during a heat wave. The latest CIBSE TM59 standard [48] on overheating in residential buildings recommends two assessment criteria to be met simultaneously: a/when overheating occurs—an adaptive overheating threshold based on adaptive comfort for living and sleeping areas with a limit on the number of hours the temperature limit is exceeded by min. 1 K, based on a 24 h moving weighted average outdoor temperature, for 3% of the occupied hours between May and September, and b/static—a limit temperature of 26 °C for sleeping hours, which must not be exceeded for more than 1% of the total hours throughout the year assumed to be sleeping hours (between 10 p.m. and 7 a.m.), i.e., 32 h per year. The risk of overheating can be reliably estimated by monitoring over 3 months (June to August) [5]. For practical reasons, the authors of many studies on overheating in buildings also use a fixed limit for living rooms, in which case it is assumed to be 28 °C [49].

In order to verify the quantitative differences in the thermal behavior of the different types of rooms in the two buildings B1 and B2, an analysis of temperature exceedances of the limit temperature threshold according to CIBSE TM52 [47] was applied. The results of the tests carried out in these buildings were related to temperature exceedances of 26 °C in bedrooms and 28 °C in living rooms, using Criterion 1 for overheating of dwellings. It is based on an acceptable percentage of hours during which the temperature limit (He) is exceeded. With this criterion, it is relatively easy to assess the time during which buildings are overheated, but it does not allow an assessment of the intensity of the phenomenon. The period analyzed was from 1 June to 31 August 2019. The number of hours against which the number of hours exceeding the limit values was compared was, unlike in the CIBSE recommendations, related to the total number of measured hours, as the aim was not to determine the design conditions for the operation of the buildings but to assess, among other things, the external climate or the passive strategy used. The hours of use were assumed to be between 22:00 and 7:00 for the bedroom and between 7:00 and 22:00 for the living room.

Figure 6 shows the hours of temperature exceedance for individual rooms in the surveyed buildings (He) and the percentage of this exceedance of He [%]. A common scale has been used in the following graphs: 1000 h and 100%.

In the B1 house, there were no temperature exceedances in either the bedrooms or the living room. In the lightweight house (B2), temperature exceedances were very similar in all bedrooms, with 76.1%, 73.7%, and 74.4% of the time in bedrooms 3, 4, and 6, respectively, and 59.6% in the living room. The amount of energy required to keep the temperature below the limit in all rooms was completely eliminated.

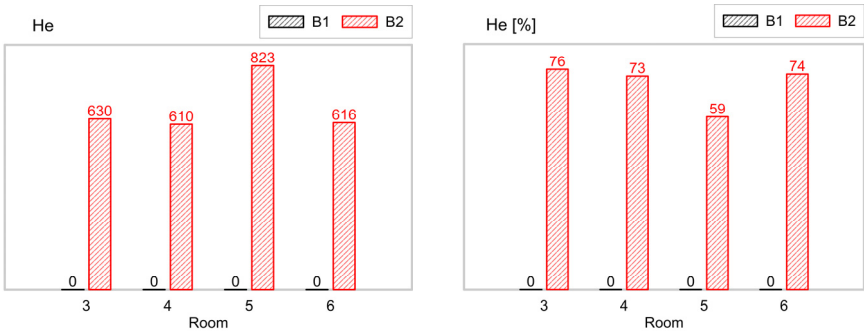

Figure 6. He values for bedrooms (rooms 3, 4, and 6) and living room (room 5) and the percentage time it is exceeded in buildings B1 and B2 for the period 1 June–31 August 2019. Bedrooms—duration of use 828 h, living room—1380 h.

3.3. Comparison between Experimental and Simulation Results

Table 6 presents results obtained from measurements and computer simulations during the period of June-August in the form of indicators such as RMSE [°C], CvRMSE [%], and Pearson's linear correlation coefficient (r).

Table 6. Statistical analysis indicators for the results of experimental measurements and numerical simulations in buildings B1 and B2 for the period 1 June–31 August 2019.

Room			B1 Building			B2 Building		
Nr	**Room Type**	**Orientation**	**r**	**RMSE**	**Cv (RMSE)**	**r**	**RMSE**	**Cv (RMSE)**
			-	**[°C]**	**[%]**	**-**	**[°C]**	**[%]**
3	Bedroom	E	0.88	0.61	2.7	0.97	2.17	7.8
4	Bedroom	S	0.89	0.56	2.5	0.98	1.70	6.1
5	Living Room	S-W	0.89	0.60	2.6	0.98	0.84	3.0
6	Bedroom	W	0.89	0.53	2.4	0.98	1.93	6.9

For the living rooms of buildings B1 and B2, the numerical simulation data are in good agreement with the experimental data for the three-month measurement period, with correlation coefficients r ranging from 0.89 to 0.98, RMSE ranging from 0.56 to 1.70 °C and Cv(RMSE) ranging from 2.6 to 3.0%. The simulation results for the west bedroom better reflect the measured temperature values in building B1 with a correlation coefficient r of 0.89, RMSE of 0.53 °C, and Cv(RMSE) of 2.4%.

In the west bedroom of building B2, despite the higher linear correlation coefficient of r = 0.98, the temperature values obtained from the simulation are significantly lower than the measured values, resulting in a mean squared error of 1.93 °C and a proportionally higher Cv(RMSE) of 6.9%. As a result, the temperature differences between these rooms in the two buildings obtained by simulation are smaller than those obtained by measurement.

The results of the calibration carried out are presented in Figures 7 and 8 and in Table 7.

The table summarizes the most important statistical analysis indicators for the results of the experimental measurements and numerical simulations in the bedrooms and living room of buildings B1 and B2 in the period 1 June–31 August 2019 obtained as a result of the model calibration.

The mean squared error and the coefficient of variation of the mean squared error of the calibrated model for the west bedroom in buildings B2 and B1 in summer 2019 were 0.94 °C and 3.4%, and 0.89 °C and 2.3% for building B1, respectively. The agreement between the experimental and simulated data obtained as a result of the calibration can be considered good in light of other research results on the evolution of indoor temperatures in buildings [33,44,50,51].

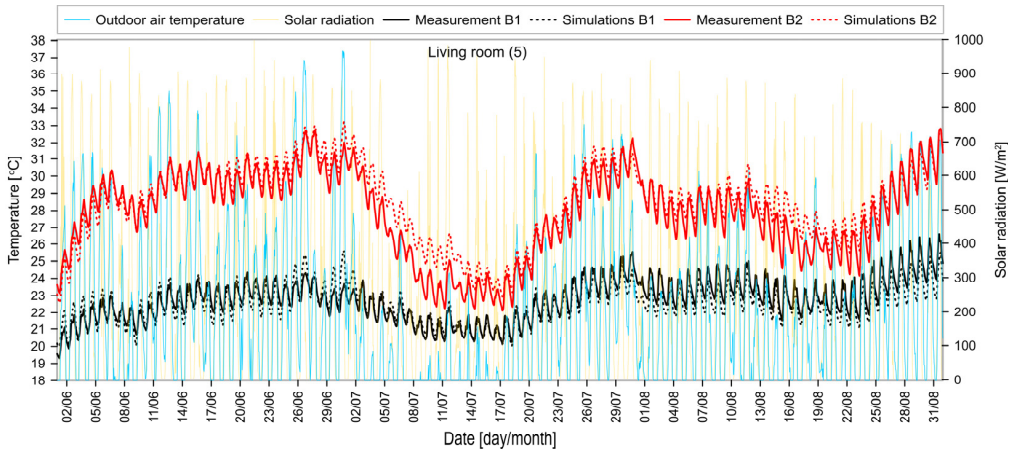

Figure 7. Hourly indoor temperature values in the living room of buildings B1 and B2 for the period June–August 2019 as obtained from experimental measurements and computer simulations.

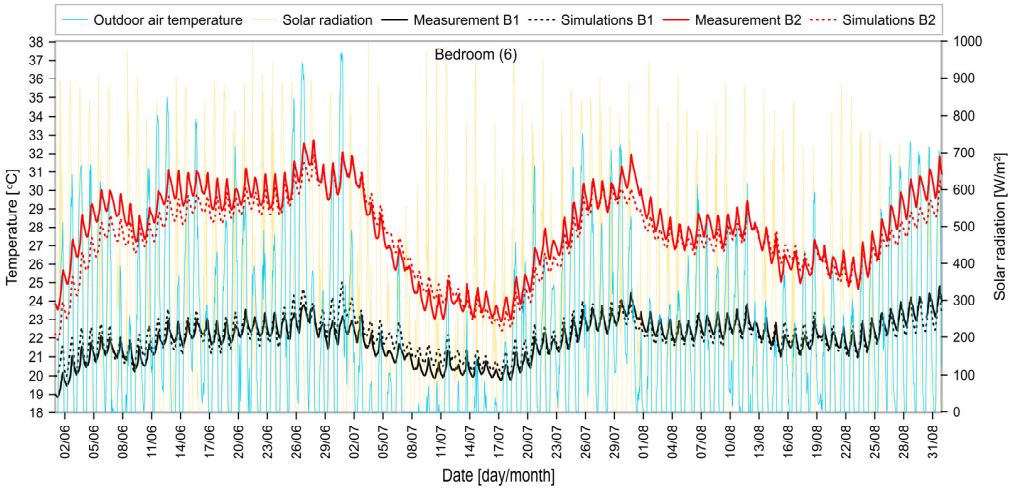

Figure 8. Hourly indoor temperature values in the western bedroom of buildings B1 and B2 for the period June–August 2019 as obtained from experimental measurements and computer simulations.

Table 7. Statistical analysis indices for the results of experimental measurements and numerical simulations in buildings B1 and B2 for the period 1 June–31 August 2019 (after model calibration).

Room			B1 Building			B2 Building		
Nr	**Room Type**	**Orientation**	**r**	**RMSE**	**Cv (RMSE)**	**r**	**RMSE**	**Cv (RMSE)**
			-	**[°C]**	**[%]**	**-**	**[°C]**	**[%]**
3	Bedroom	E	0.88	0.58	2.6	0.93	1.10	3.9
4	Bedroom	S	0.90	0.55	2.4	0.95	0.78	2.8
5	Living Room	S-W	0.90	0.60	2.6	0.96	0.94	3.4
6	Bedroom	W	0.89	0.51	2.3	0.94	0.94	3.4

3.4. Effect of Internal Heat

Figures 9 and 10 show the hourly temperature profiles from 1 June to 31 August 2019 obtained by modeling in Energy Plus for the living room and west bedroom, respectively, after accounting for heat gains from occupants. As can be seen by comparing Figures 7 and 8 with Figures 9 and 10, assuming a uniform heat load of 5 W/m^2 [24], the indoor temperature of the analyzed rooms in both buildings increased by approximately 2 °C.

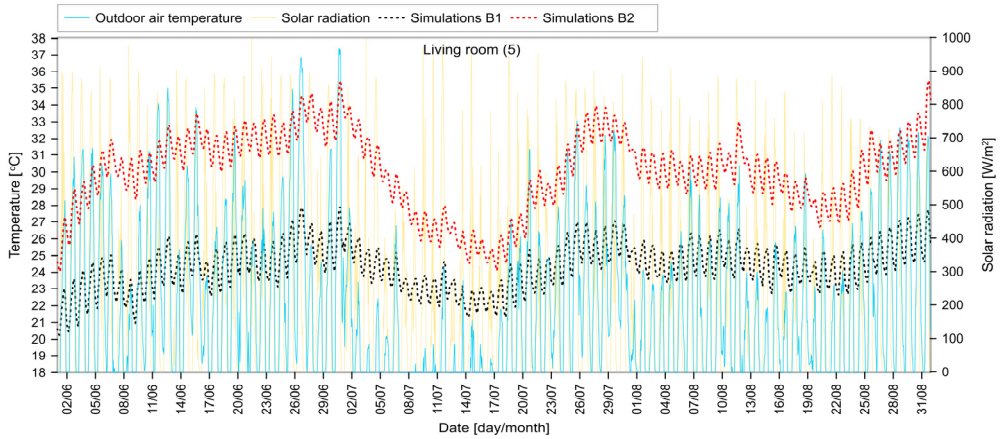

Figure 9. Hourly indoor temperature values in the living room (Room 5) of buildings B1 and B2 for the period 1 to 30 June 2019 as obtained from computer simulations (considering the heat generated by the user, after calibration).

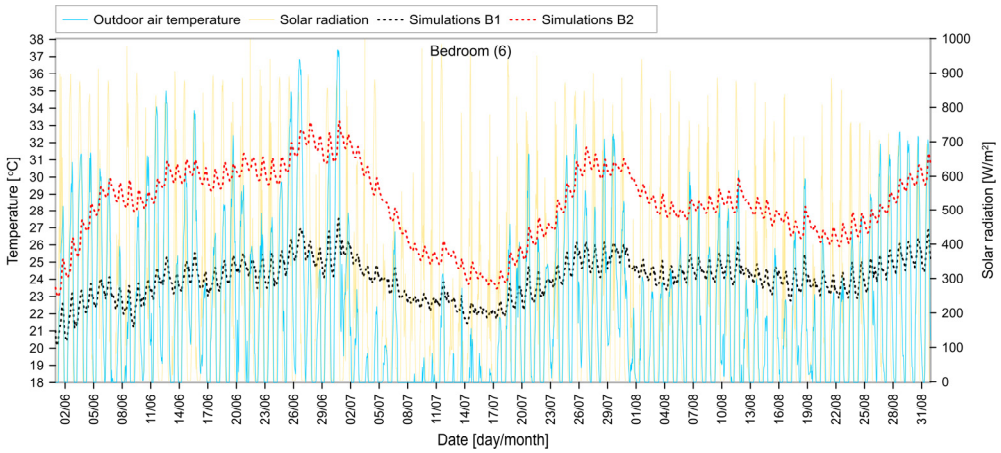

Figure 10. Hourly indoor temperature values in the living room (Room 6) of buildings B1 and B2 for the period 1 to 30 June 2019 as obtained from computer simulations (considering the heat generated by the user, after calibration).

Figure 11 shows the hours of temperature exceedance for each room in the buildings studied (He) and the percentage of this exceedance of He [%]. The same scale has been used in both graphs below: 1000 h and 100%.

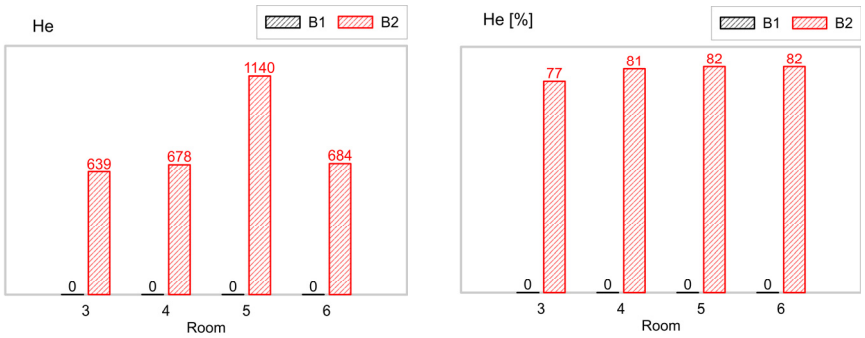

Figure 11. The He values for the bedrooms (Rooms 3, 4, and 6) and the living room (Room 5) and the percentage of time they are exceeded in buildings B1 and B2 for the period 1 June–31 August 2019, taking into account the heat gains from the occupants. Time of use: bedrooms −828 h, living room 1380 h.

In building B1, the temperatures in the living room and bedrooms were not exceeded when occupant heat gains were taken into account. In building B2, the temperatures in the west, south, and east bedrooms exceeded the threshold for 684 h or 82.6% of the time, 678 h or 81.8% of the time, and 639 or 77.2% of the time, respectively. In the living room, the temperature was exceeded for 1140 h or 82.6% of the time.

4. Discussion

4.1. Risk of Building Overheating

For the period from 1 June to 31 August 2019, the average outdoor temperature was 20.9 °C, which was 3.5 °C above the multi-year average. The temperature during this period was in line with the temperature projection for the end of the 21st century under the IPCC 6.0 scenario. For the whole period considered, the average temperature in the bedrooms of building B1 was 4.3 °C lower in the bedrooms and 5.7 °C lower in the living room. During the June 2019 heat wave, the average outdoor air temperature was 22.7 °C, 6.6 °C higher than the multi-year average for June in Zielona Góra, more than 1 °C higher than the average air temperature for this month in Rome, and almost 2 °C higher than the worst case IPCC8.5—Hot scenario for the year 2100. The average minimum night temperature in the bedrooms of buildings B1 and B2 was 23.5 °C and 30.2 °C, respectively, after accounting for heat gain from the occupants. In the living rooms, the corresponding average maximum temperatures were 24.6 °C and 31.9 °C. During the June heat wave, the minimum night temperature in building B1 was on average 6.7 °C lower, and the maximum day temperature was 7.3 °C lower than in building B2. In building B2, the temperatures in the west, south, and east bedrooms exceeded the threshold for 684 h or 82.6% of the time, 678 h or 81.8% of the time, and 639 or 77.2% of the time, respectively. In the living room, the temperature was exceeded for 1140 h or 82.6% of the time. The temperature in the bedrooms of building B1 did not exceed 26 °C and in the living room 28 °C at any time between 1 June and 31 August 2019. By removing the floor insulation and increasing the thermal mass of the walls from light to medium, the need for mechanical cooling was eliminated.

As there are no examples in the literature of an analysis of the thermal performance of energy-efficient residential buildings with uninsulated floors, the authors referred to the results obtained from vernacular buildings, often using earth-rammed wall solutions. However, when comparing the results obtained, it should be borne in mind that vernacular buildings are characterized by significantly poorer thermal insulation of the building envelope than the building analyzed in this study. For the B1 building, the values of the heat transfer coefficient U (calculated using the F-factor and a fictitious insulation layer [38]) and the ventilation loss coefficient (calculated using an assumed recuperative heat exchanger with 75% efficiency) per square meter of the floor were 0.585 W/m^2 floor × K and 0.396 W/m^2 floor × K, respectively. Thus the total heat loss coefficient for building B1 calculated as the sum of conductive and ventilation losses [52] had a value similar to the average values for recent residential projects in London: 0.83 W/m^2 floor × K for Mint, 0.79 W/m^2 floor × K for Angel Waterside, 1.01 W/m^2 floor × K for Adelaide Wharf [52].

In the study, with an average outdoor temperature of 22.7 °C in June 2019, the average indoor temperatures in the three bedrooms and living room of building B1 were 23.9 °C and 24.2 °C respectively, 1.2 °C higher. In a study conducted in a detached house in the municipality of Tabuaço in northern Portugal (Csb according to the Köppen climate classification), Fernandes et al. [53] recorded an average temperature of 23.9 °C in the ground floor living room, with an average outdoor temperature 0.5 °C higher throughout the summer of 2014. Thus, both buildings were similarly effective against high indoor temperatures. In the southern Italian towns of Sassi of Matera and Trulli of Alberobello, the ability of vernacular buildings to provide thermal comfort to residents during periods of high temperatures was demonstrated by Cardinale et al. [54]. The results of the model tests, verified by experimental measurements carried out in both buildings, showed that

during the summer season (May–September) the indoor temperatures remained within the comfort limits, not exceeding 28 °C, even when the outdoor air temperatures were high, exceeding 35 °C.

Significantly higher indoor temperatures in a building with an uninsulated floor and heavy wall and roof solutions, under climatic conditions similar to those of Fernandes et al. [53], were obtained by Roque et al. [55], in a study carried out in the summer of 2020 in a free-standing experimental room, in Albergaria-a-Velha, (central coastal region of Portugal (Csb climate, according to the Köppen-Geiger classification), with an average outdoor temperature of 23–23.5 °C, the indoor temperature varied between 25–27 °C. The higher indoor temperatures may have been due to the much lower total thermal capacity of the monitored room, which was a single-room building, compared to the much larger multi-room buildings in this study and in [53].

The authors also compared their findings with those of other authors who analyzed the potential benefits of combining the main passive cooling strategies in the temperate climate.

A modeling study of the effectiveness of the simultaneous use of several different passive measures to reduce the risk of overheating in hot weather for a late 19th-century Victorian terraced house in southeast England was carried out by Porritt et al. [56]. By combining passive measures such as loft and roof insulation, reducing the solar absorptivity of the walls and roof, turning on external blinds, changing the way windows are opened, and leaving them open for night ventilation, they achieved a reduction in peak temperatures of 4.6 °C in the living rooms and 4 °C in the master bedroom.

O'Donovan et al. [43] modeled the effect of a passive cooling strategy for an office building in Budapest. The average indoor temperature reduction achieved with the combined use of night ventilation and solar shading was 2.9–3.5 °C in summer under current and future conditions. The combination of solar shading and night ventilation currently provides full thermal comfort, but the IPCC 8.5 worst-case scenario requires additional active cooling by 2050, with cooling energy savings of around 90%.

Silva et al. [21] showed that the simultaneous use of night ventilation and window shading under IPCC scenario 4.5 has a maximum theoretical potential to reduce national cooling energy demand in residential buildings in Switzerland by 84% by 2049.

In south-facing experimental rooms on the top floor of a research center in Nowy Kisielin near Zielona Góra, Kuczyński et al. [7] studied the effects of different scenarios for the use of three passive cooling methods: thermal capacity, night ventilation, and external blinds on indoor temperature during intense heat waves in 2019. While the use of a high thermal mass envelope combined with night ventilation reduced the cooling energy demand by 92.5%, the addition of a third passive measure—external blinds—reduced the average peak temperature by 7.4 °C during the day and 6.3 K at night. As a result, no mechanical cooling was required.

4.2. Impact of Thermal Insulation Removal from the Building Floor on Heating Energy Demand

The calculated heating energy demand in the 2019/2020 heating period for buildings B1 and B2 was 6347.1 kWh and 5130.6 kWh respectively, i.e., 51.9 kWh/m^2 and 42.0 kWh/m^2 per 1 m^2 floor. The annual calculated heating energy demand for a building without floor insulation was 23.7% higher than for a building with an insulated floor.

The actual differences in energy demand between the two buildings studied were expected to be even smaller, as the results show that heat loss by floor can be substantially reduced by using vertical external insulation of the foundation wall [57,58]. Goldberg and Mosiman [58], applying R-10 XPS insulation up to half the wall height below ground level, achieved a 5% reduction in energy demand for a detached single-story building in Duluth, MN, USA. Liu et al. [59] in an experimental study conducted in full-scale single-room test facilities at the University of Newcastle, Australia, using vertical XPS insulation 42 cm deep and 3 cm thick, achieved a reduction in annual energy demand per square meter of floor space of 7.3 kWh/m^2. In this study, 80 cm deep and 20 cm thick vertical polystyrene foam

was used around the foundations. The actual heating energy consumption in 2019/2020 for buildings B1 and B2 was 6168.7 kWh and 5499.6 kWh, respectively. The actual consumption for building B1 was 5.5 kWh/m^2 per 1 m^2 floor or 12.5% higher than for B2, which is almost twice as low as calculated.

In Poland, as in other temperate climate EU countries, building regulations do not allow the use of uninsulated floors at ground level in newly designed and constructed buildings. In Spain, thermal insulation of ground floors is required in new residential buildings, even in regions with the mildest winters [60]. In Portugal, which has a warmer climate than Poland, uninsulated floors on the ground floor of residential buildings are common and meet the requirements of Portuguese regulations on the energy performance of buildings [55,61]. The higher temperatures in Tabuaço, in the north of Portugal, occur in the summer. In winter, the differences are much smaller. During the heating period of the year 2019/2020, the average value of outdoor temperatures in Zielona Góra was 4.9 °C, compared to 5.0 °C in Tabuaço [53].

The reasons for the relatively small increase in energy demand caused by the removal of the floor insulation are further explained by the ground temperature distribution shown in Figure 12.

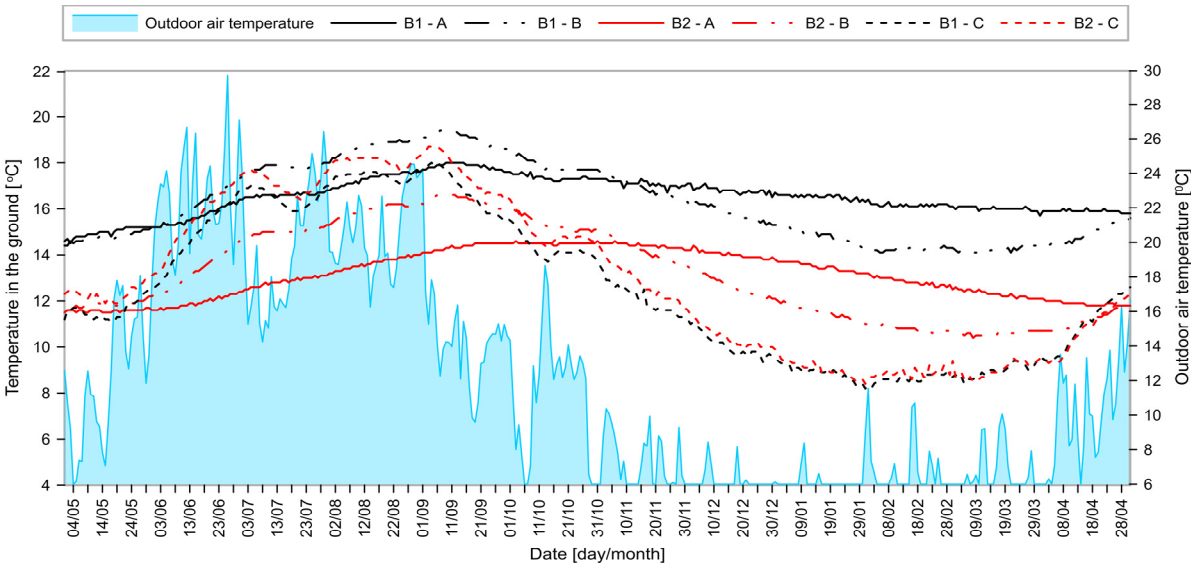

Figure 12. Daily values of outdoor air and ground temperatures under the floor slab of buildings B1 and B2 at depths of 1.5 m for the period 1 May 2019 to 30 April 2020.

The graph shows the course of temperatures in the ground under the floor slab of buildings B1 and B2 at a depth of 1.5 m for the period 1 May 2019 to 30 April 2020. The temperature values in buildings B1 and B2 are shown in black and red, respectively. The solid, dashed, and dotted lines show the temperature values at the measuring points located in the center of the building (point A), 0.5 m from the external wall to the inside of the building (point B), and 0.5 m from the external wall to the outside of the building (point C). The highest temperatures in the soil under Building B1 occurred in early September, immediately after the end of the August heat wave. The lowest temperatures for each of the measurement locations were recorded at different times. At the end of January, the minimum temperature of 8 °C was reached at monitoring location C. At location B, the lowest temperature of around 14 °C lasted for almost 1.5 months, from the end of January to mid-March. At location A, the lowest temperature of about 16 °C lasted for about 3.5 months, from the end of January to mid-May.

A comparison of the soil temperatures under the buildings can lead to interesting observations. Over the whole measurement period, the average ground temperatures were higher for building B1 by about 3.5–4 °C at measurement location A and by 2.5–3.5 °C at

measurement location B. At location C, the ground temperatures differed slightly. This distribution of soil temperatures indicates that the volume of soil under the building, at least to a depth of 1.5 m becomes a large heat accumulator, helping to reduce excessive building temperatures in summer and reducing soil heat loss during the heating period.

4.3. Energy Policy for the Design of Building

Over the past three decades, policies to improve the energy efficiency of buildings have been implemented around the world. As a result, most countries with temperate climates now have standards aimed at reducing energy consumption during the heating season. New increasingly stringent standards are being introduced for the thermal insulation and airtightness of existing homes. Consequently, some studies indicate that the combination of high levels of thermal insulation and airtightness in energy-efficient, passive, or near-zero-energy buildings may lead to an increased risk of overheating compared to older buildings [52,62–64]. Other studies show that although there is no direct correlation between a building's level of energy efficiency and its susceptibility to overheating, the effectiveness of passive overheating control systems in more energy-efficient buildings is strongly linked to the behavior of the building occupants [2,40,65], which often differ significantly from those expected [66,67]. However, there is growing evidence that in temperate climates, where both average summer temperatures and the frequency and intensity of heat waves are increasing, designing new buildings and retrofitting existing ones to be more energy efficient during the heating season is not enough [67,68]. On the basis of long-term weather forecasts, Rahif et al. [14] use the example of terraced housing in the municipality of Woluwe-Saint-Lambert in Brussels to show that regions that are currently dominated by heating could become dominated by cooling in the next decades. Even in an optimistic scenario of IPCC 4.5 emissions in a heating-dominated region like Brussels by the end of the century, cooling degree-days will equal heating degree-days [14]. The authors argue that the current approach of building design in these regions should be changed, as it could lead to an increase in overall energy consumption in the future, while at the same time increasing the risk of buildings overheating.

The analysis presented in this paper shows that, under the conditions of climate change related to global warming, existing regulations that set specific standards for individual building elements, e.g., maximum heat transfer coefficients for walls, ceilings, or floors, rather than, for example, average values for heat transfer coefficient and annual energy demand per m^2 of building floor area, or the amount of CO_2 emitted by the building per year, can make it difficult or impossible to introduce solutions that would work in sustainable energy-efficient and resilient building.

The proposed passive cooling concept is in line with the new approach to building design described above, which should not be limited to reducing thermal energy demand, but should also respond to the needs arising from global warming [14,52,68], as well as the use of new technologies based mainly on the use of non-conventional energy sources [69,70].

5. Conclusions

The effectiveness of a passive cooling strategy by increasing the thermal capacity of the walls of a detached single-family house and ensuring heat exchange between the floor and the ground underneath by removing the floor insulation was evaluated during the hottest summer in Poland and many other European countries in 2019.

The passive methods used proved very effective in improving both daytime and night-time comfort, reducing daytime peak temperatures during heat waves by 5.2 °C to 7.1 °C and night-time peak temperatures by 4.7 °C to 6.8 °C. It was found that at temperatures forecast in the worst-case scenario for the temperate climate of central and eastern Europe for the year 2100, such a strategy would completely eliminate the need for mechanical cooling. Experimental studies showed that this was achieved when occupant heat gains were not taken into account. Modeling studies have shown that the need for mechanical cooling will also be eliminated when occupant heat gains are taken into account at a

moderate level. Avoiding the need for mechanical cooling of buildings is crucial given the expected increase in power outages in temperate climates due to increasing heat waves, and the additional increase in anthropogenic heat emissions due to waste heat from air conditioning and air removed from buildings by ventilation, and consequently night-time temperatures when renewable energy generation from photovoltaic systems is not possible.

After model calibration, the calculated temperatures in all bedrooms, east, south, and west, and in the living room of both buildings were in good agreement with their values from experimental measurements.

In addition to checking the effectiveness of the strategies used in summer, their impact on energy consumption during the heating period was also checked, which showed that they led to an increase in energy consumption of 5.5 kWh/m^2 of building floor area in 2019/2020. The theoretical analysis and the experimental tests in 2019/2020 show that after the removal of the insulation from the floor at ground level, the value of the total heat loss coefficient, calculated as the sum of conduction and ventilation losses per square meter of the floor in the analyzed building, was at a level close to that of recently developed residential projects.

The distribution of temperatures underneath the floor over the period 1 May 2019–30 April 2020 shows that, to a depth of well below 1.5 m, with the exception of zones adjacent to foundations under external walls, it becomes a heat accumulator that reduces excessive building temperatures in summer and reduces heat loss to the soil during the heating period. It also shows that the additional heating energy demand can be reduced by using horizontal insulation on the outside of the building and in the strip next to the external walls. With good insulation of the roof, external walls, and windows of a building, in combination with the use of mechanical ventilation with heat recovery, such a building can meet the criteria of a near-zero energy building.

The analysis presented in this paper shows that, under the conditions of climate change related to global warming, existing regulations that set specific standards for individual building elements, e.g., maximum heat transfer coefficients for walls, ceilings, or floors, rather than, for example, average values for heat transfer coefficient and annual energy demand per m^2 of building floor area, or the amount of CO_2 emitted by the building per year, can make it difficult or impossible to introduce solutions that would work in sustainable, energy-efficient, resilient building.

The proposed cooling passive measures are in line with the new approach to building design proposed in recent years, which, according to some authors, should not be limited to reducing heating energy demand, but should also respond to the needs arising from global warming as well as the use of new technologies based mainly on the use of non-conventional energy sources.

Author Contributions: Conceptualization, T.K. and A.S.; methodology, A.S.; formal analysis, T.K. and A.S.; investigation, A.S.; numerical simulations, A.S.; resources, T.K. and A.S.; data analysis T.K. and A.S., data curation, A.S.; writing—original draft preparation, T.K. and A.S.; writing—review and editing, T.K. and A.S.; visualization, A.S.; supervision, T.K. All authors have read and agreed to the published version of the manuscript.

Funding: This research received no external funding.

Data Availability Statement: Data are contained within the article.

Conflicts of Interest: The authors declare no conflict of interest.

Abbreviations

IPCC	Intergovernmental Panel on Climate Change
TMP	Thermal Mass Parameter [kJ/m^2 K]
TFA	Total Floor Area [m^2]
RMSE	root mean square error [°C]

Cv(RMSE)	root mean square coefficient of variation [%]
A	area [m^2]
U	thermal transmittance [W/m^2 K]
T_o	outdoor air temperature [°C]
T_i	indoor air temperature [°C]
T_m	temperature of internal air measured [°C]
T_c	temperature of internal air calculated [°C]
N	number of measurements
T_{min}	minimum temperature [°C]
T_{max}	maximum temperature [°C]
T_{av}	average temperature [°C]
Trm	exponentially weighted running mean outdoor air temperature [°C]
$\Delta\theta_o$	outdoor air temperature difference [°C]
$\Delta\theta_i$	indoor air temperature difference [°C]
r	Pearson's linear correlation coefficient [-]
He	temperature exceedance [h] or [%]

References

1. Chapman, S.C.; Watkins, N.; Stainforth, D.A. Warming trends in summer heatwaves. *Geophys. Res. Lett.* **2019**, *46*, 1634–1640. [CrossRef]
2. Dartevelle, O.; Altomonte, S.; Masy, G.; Mlecnik, E.; Van Moeseke, G. Indoor summer thermal comfort in a changing climate: The case of a nearly zero energy house in wallonia (Belgium). *Energies* **2022**, *15*, 2410. [CrossRef]
3. NOAA. *2021 Was World's 6th-Warmest Year on Record*; National Oceanic and Atmospheric Administration: Washington, DC, USA, 2022. Available online: https://www.noaa.gov/news/2021-was-worlds-6th-warmest-year-on-record (accessed on 4 July 2023).
4. Hollis, D.; McCarthy, M.; Kendon, M.; Legg, T.; Simpson, I. HadUK-Grid—A new UK dataset of gridded climate observations. *Geosci. Data J.* **2019**, *6*, 151–159. [CrossRef]
5. Lomas, K.J.; Watson, S.; Allinson, D.; Fateh, A.; Beaumont, A.; Allen, J.; Foster, H.; Garrett, H. Dwelling and household characteristics' influence on reported and measured summertime overheating: A glimpse of a mild climate in the 2050′s. *Build. Environ.* **2021**, *201*, 107986. [CrossRef]
6. Baker, S. *Europe Is Battling an Unprecedented Heat Wave, Which Has Set Records in 3 Countries and Is Linked to at Least 4 Deaths*; Business Insider; Insider Inc.: New York, NY, USA, 2019.
7. Kuczyński, T.; Staszczuk, A.; Gortych, M.; Stryjski, R. Effect of thermal mass, night ventilation and window shading on summer thermal comfort of buildings in a temperate climate. *Build. Environ.* **2021**, *204*, 108126. [CrossRef]
8. Murage, P.; Hajat, S.; Kovats, R.S. Effect of night-time temperatures on cause and age-specific mortality in London. *Environ. Epidemiol.* **2017**, *1*, e005. [CrossRef]
9. Arbuthnott, K.G.; Hajat, S. The health effects of hotter summers and heat waves in the population of the United Kingdom: A review of the evidence. *Environ. Health Glob. Access Sci. Source* **2017**, *16*, 119. [CrossRef]
10. Quinn, A.; Tamerius, J.D.; Perzanowski, M.; Jacobson, J.S.; Goldstein, I.; Acosta, L.; Shaman, J. Predicting indoor heat exposure risk during extreme heat events. *Sci. Total Environ.* **2014**, *490*, 686–693. [CrossRef] [PubMed]
11. Climate Centre. European Summer Heatwaves the Most Lethal Disaster of 2019, Says International Research Group. 5 May 2020. Available online: https://www.climatecentre.org/565/european-summer-heatwaves-the-most-lethal-disaster-of-2019-says-international-research-group/ (accessed on 4 July 2023).
12. Climate Centre. New Official Data in Europe Exposes Heatwaves as Still the 'Silent Killer' of the Elderly. 9 September 2019. Available online: https://www.climatecentre.org/737/new-official-data-in-europe-exposes-heatwaves-as-still-the-a-silent-killera-of-the-elderly/ (accessed on 4 July 2023).
13. Carrington, D. Heatwaves in 2019 Led to Almost 900 Extra Deaths in England. *The Guardian*. 7 January 2020. Available online: https://www.theguardian.com/world/2020/jan/07/heatwaves-in-2019-led-to-almost-900-extra-deaths-in-england (accessed on 10 June 2022).
14. Rahif, R.; Kazemi, M.; Attia, S. Overheating analysis of optimized nearly Zero-Energy dwelling during current and future heatwaves coincided with cooling system outage. *Energy Build.* **2023**, *287*, 112998. [CrossRef]
15. Raddatz, B. *Almost 500 Heat Deaths in Berlin Last Year*; Robert Koch Institute: Berlin, Germany, 2019; Available online: https://www.rbb24.de/panorama/thema/2019/klimawandel/beitraege/statistik-hitzetote-sommer-2018-robert-koch-institut.html (accessed on 10 June 2022).
16. Biddle, J. Explaining the spread of residential air conditioning, 1955–1980. *Explor. Econ. Hist.* **2008**, *45*, 402–423. [CrossRef]
17. Peacock, A.D.; Jenkins, D.P.; Kane, D. Investigating the potential of overheating in UK dwellings as a consequence of extant climate change. *Energy Policy* **2010**, *38*, 3277–3288. [CrossRef]
18. Narumi, D.; Kondo, A.; Shimoda, Y. Effects of anthropogenic heat release upon the urban climate in a Japanese megacity. *Environ. Res.* **2009**, *109*, 421–431. [CrossRef] [PubMed]

19. Vahmani, P.; Luo, X.; Jones, A.; Hong, T. Anthropogenic heating of the urban environment: An investigation of feedback dynamics between urban micro-climate and decomposed anthropogenic heating from buildings. *Build. Environ.* **2022**, *213*, 108841. [CrossRef]
20. Mayrhofer, L.; Müller, A.; Bügelmayer-Blaschek, M.; Malla, A.; Kranzl, L. Modelling the effect of passive cooling measures on future energy needs for the Austrian building stock. *Energy Build.* **2023**, *296*, 113333. [CrossRef]
21. Silva, R.; Eggimann, S.; Fierz, L.; Fiorentini, M.; Orehounig, K.; Baldini, L. Opportunities for passive cooling to mitigate the impact of climate change in Switzerland. *Build. Environ.* **2022**, *208*, 108574. [CrossRef]
22. Van den Wymelenberg, K. Patterns of occupant interaction with window blinds: A literature review. *Energy Build.* **2012**, *51*, 165–176. [CrossRef]
23. Fabi, V.; Andersen, R.V.; Corgnati, S.; Olesen, B.W. Occupants' window opening behaviour: A literature review of factors influencing occupant behaviour and models. *Build. Environ.* **2012**, *58*, 188–198. [CrossRef]
24. Hamdy, M.; Carlucci, S.; Hoes, P.J.; Hensen, J.L.M. The impact of climate change on the overheating risk in dwellings—A Dutch case study. *Build. Environ.* **2017**, *122*, 307–323. [CrossRef]
25. Mantesi, E.; Hopfe, C.J.; Mourkos, K.; Glass, J.; Cook, M. Empirical and computational evidence for thermal mass assessment: The example of insulating concrete formwork. *Energy Build.* **2019**, *188–189*, 314–332. [CrossRef]
26. Tink, V.; Porritt, S.; Allinson, D.; Loveday, D. Measuring and mitigating overheating risk in solid wall dwellings retrofitted with internal wall insulation. *Build. Environ.* **2018**, *141*, 247–261. [CrossRef]
27. Kuczyński, T.; Staszczuk, A. Experimental study of the thermal behavior of PCM and heavy building envelope structures during summer in a temperate climate. *Energy* **2023**, *279*, 128033. [CrossRef]
28. Summa, S.; Remia, G.; Di Perna, C.; Stazi, F. Experimental and numerical study on a new thermal masonry block by comparison with traditional walls. *Energy Build.* **2023**, *292*, 113125. [CrossRef]
29. Kuczyński, T.; Staszczuk, A. Experimental study of the influence of thermal mass on thermal comfort and cooling energy demand in residential buildings. *Energy* **2020**, *195*, 116984. [CrossRef]
30. Staszczuk, A.; Wojciech, M.; Kuczyński, T. The effect of floor insulation on indoor air temperature and energy consumption of residential buildings in moderate climates. *Energy* **2017**, *138*, 139–146. [CrossRef]
31. GUS (Główny Urząd Statystyczny): Budownictwo w 2021 Roku. Available online: https://stat.gov.pl/obszary-tematyczne/przemysl-budownictwo-srodki-trwale/budownictwo/budownictwo-w-2021-roku,13,13.html (accessed on 15 September 2023).
32. Kottek, M.; Grieser, J.; Beck, C.; Rudolf, B.; Rubel, F. World Map of the Koppen-Geiger climate classification updated. *Meteorol. Z.* **2006**, *15*, 259–263. [CrossRef]
33. Sage-Lauck, J.S.; Sailor, D.J. Evaluation of phase change materials for improving thermal comfort in a super-insulated residential building. *Energy Build.* **2014**, *79*, 32–40. Available online: https://energyplus.net/assets/nrel_custom/pdfs/pdfs_v22.1.0/EngineeringReference.pdf (accessed on 7 August 2023). [CrossRef]
34. *EN ISO 13786:2017*; Thermal Performance of Building Components. Dynamic Thermal Characteristics. Calculation Methods. ISO: Geneva, Switzerland, 2017.
35. SAP. *The Government's Standard Assessment Procedure for Energy Rating of Dwellings*; BRE: Watford, UK, 2012; Available online: https://www.bre.co.uk/filelibrary/SAP/2012/SAP-2012_9-92.pdf (accessed on 7 August 2023).
36. EnergyPlus™ Weather File. 2022. Available online: https://energyplus.net/weather (accessed on 7 August 2023).
37. *EN ISO 6946:2017*; Building Components and Building Elements—Thermal Resistance and Thermal Transmittance—Calculation Methods. ISO: Geneva, Switzerland, 2017.
38. EnergyPlus™ Version 9.6.0 Documentation, Engineering Reference. U.S. Department of Energy, 23 September 2021. Available online: https://energyplus.net/assets/nrel_custom/pdfs/pdfs_v9.6.0/EngineeringReference.pdf (accessed on 5 January 2023).
39. Tüysüz, F.; Sözer, H. Calibrating the building energy model with the short term monitored data: A case study of a large-scale residential building. *Energy Build.* **2020**, *224*, 110207. [CrossRef]
40. Baba, F.M.; Ge, H.; Zmeureanu, R.; Wang, L. Calibration of building model based on indoor temperature for overheating assessment using genetic algorithm: Methodology, evaluation criteria, and case study. *Build. Environ.* **2022**, *207 Pt B*, 108518C. [CrossRef]
41. Lozinsky, C.H.; Touchie, M. Improving energy model calibration of multi-unit residential buildings through component air infiltration testing. *Build. Environ.* **2018**, *134*, 218–229. [CrossRef]
42. Carlon, E.; Schwarz, M.; Golicza, L.; Verma, V.K.; Prada, A.; Baratieri, M.; Haslinger, W.; Schmidl, C. Efficiency and operational behaviour of small-scale pellet boilers installed in residential buildings. *Appl. Energy* **2015**, *155*, 854–865. [CrossRef]
43. O' Donovan, A.; Murphy, M.D.; O'Sullivan, P.D. Passive control strategies for cooling a non-residential nearly zero energy office: Simulated comfort resilience now and in the future. *Energy Build.* **2021**, *231*, 110607. [CrossRef]
44. Jamil, H.; Alam, M.; Sanjayan, J.; Wilson, J. Investigation of PCM as retrofitting option to enhance occupant thermal comfort in a modern residential building. *Energy Build.* **2016**, *133*, 217–229. [CrossRef]
45. Artmann, N.; Manz, H.; Heiselberg, P. Climatic potential for passive cooling of buildings by night-time ventilation in Europe. *Appl. Energy* **2007**, *84*, 187–201. [CrossRef]
46. *ASHRAE Standard 55*; Thermal Environmental Conditions for Human Occupancy. ASHRAE: Peachtree Corners, GA, USA, 2017.
47. *CIBSE TM52*; The Limits of Thermal Comfort-Avoiding Overheating in European Buildings. CIBSE: London, UK, 2013.
48. *CIBSE TM59*; Design Methodology for the Assessment of Overheating Risk in Homes. CIBSE: London, UK, 2017.

49. Psomas, T.; Heiselberg, P.; Duer, K.; Bjørn, E. Overheating risk barriers to energy renovations of single family houses: Multicriteria analysis and assessment. *Energy Build.* **2016**, *117*, 138–148. [CrossRef]
50. O' Donovan, A.; O'Sullivan, P.D.; Murphy, M.D. Predicting air temperatures in a naturally ventilated nearly zero energy building: Calibration, validation, analysis and approaches. *Appl. Energy* **2019**, *250*, 991–1010. [CrossRef]
51. Coakley, D. Calibration of Detailed Building Energy Simulation Models to Measured Data Using Uncertainty Analysis. Ph.D. Thesis, National University of Ireland, Dublin, Ireland, 2014.
52. Yannas, S.; Rodríguez-Álvarez, J. Domestic overheating in a temperate climate: Feedback from London Residential Schemes. *Sustain. Cities Soc.* **2020**, *59*, 102189. [CrossRef]
53. Fernandes, J.; Pimenta, C.; Mateus, R.; Silva, S.M.; Bragança, L. Contribution of Portuguese Vernacular Building Strategies to Indoor Thermal Comfort and Occupants' Perception. *Buildings* **2015**, *5*, 1242–1264. [CrossRef]
54. Cardinale, N.; Rospi, G.; Stefanizzi, P. Energy and microclimatic performance of Mediterranean vernacular buildings: The Sassi district of Matera and the Trulli district of Alberobello. *Build. Environ.* **2013**, *59*, 590–598. [CrossRef]
55. Roque, E.; Vicente, R.; Almeida, R.M.S.F.; Ferreira, V.M. The Impact of Thermal Inertia on the Indoor Thermal Environment of Light Steel Framing Constructions. *Energies* **2022**, *15*, 3061. [CrossRef]
56. Porritt, S.; Shao, L.; Cropper, P.; Goodier, C. Adapting dwellings for heat waves. *Sustain. Cities Soc.* **2011**, *1*, 81–90. [CrossRef]
57. Cox-Smith, I. *Perimeter Insulation of Concrete Slab Foundations*; BRANZ: Judgeford, New Zealand, 2016.
58. Goldberg, L.; Mosiman, G. *High-Performance Slab-on-Grade Foundation Insulation Retrofits*; National Renewable Energy Laboratory (NREL): Golden, CO, USA, 2015. [CrossRef]
59. Liu, Z.; Alterman, D.; Page, A.; Moghtaderi, B.; Chen, D. An experimental study on the thermal effects of slab-edge-insulation for slab-on-grade housing in a moderate Australian climate. *Energy Build.* **2021**, *235*, 110675. [CrossRef]
60. Royal Decree 732/2019 of 20 December, Modifying the Technical Building Code, Approved by Royal Decree 314/2006 of 17 March (Real Decreto 732/2019, de 20 de Diciembre, por el que se Modifica el Código Técnico de la Edificación, Aprobado por Real Decreto 314/2006, de 17 de Marzo). 2019. Available online: https://www.boe.es/boe/dias/2019/12/27/pdfs/BOE-A-2019-18528.pdf (accessed on 28 July 2023).
61. Roque, E.; Vicente, R.; Almeida, R.M. Opportunities of Light Steel Framing towards thermal comfort in southern European climates: Long-term monitoring and comparison with the heavyweight construction. *Build. Environ.* **2021**, *200*, 107937. [CrossRef]
62. Goia, F.; Time, B.; Gustavsen, A. Impact of opaque building envelope configuration on the heating and cooling energy need of a single family house in cold climates. *Energy Proceeding* **2015**, *78*, 2626–2631. [CrossRef]
63. Costanzo, V.; Fabbri, K.; Piraccini, S. Stressing the passive behavior of a Passivhaus: An evidence-based scenario analysis for a Mediterranean case study. *Build. Environ.* **2018**, *142*, 265–277. [CrossRef]
64. Ibrahim, A.; Pelsmakers, S. Low-energy housing retrofit in North England: Overheating risks and possible mitigation strategies. *Build. Serv. Eng. Res. Technol.* **2018**, *39*, 161–172. [CrossRef]
65. Taylor, J.; McLeod, R.; Petrou, G.; Hopfe, C.; Mavrogianni, A.; Castaño-Rosa, R.; Pelsmakers, S.; Lomas, K. Ten questions concerning residential overheating in Central and Northern Europe. *Build. Environ.* **2023**, *234*, 110154. [CrossRef]
66. Mavrogianni, A.; Pathan, A.; Oikonomou, E.; Biddulph, P.; Symonds, P.; Davies, M. Inhabitant actions and summer overheating risk in London dwellings. *Build. Res. Inf.* **2017**, *45*, 119–142. [CrossRef]
67. Lomas, K.J.; Porritt, S.M. Overheating in buildings: Lessons from research. *J. Build. Res. Inf.* **2017**, *45*, 1–18. [CrossRef]
68. Rui, B.; Wen-Shao, C.; Yang, Y.; Yitong, X.; Haibo, G. Overheating of residential buildings in the severe cold and cold regions of China: The gap between building policy and performance. *Build. Environ.* **2022**, *225*, 109601. [CrossRef]
69. Norouzi, M.; Haddad, A.N.; Jiménez, L.; Hoseinzadeh, S.; Boer, D. Carbon footprint of low-energy buildings in the United Kingdom: Effects of mitigating technological pathways and decarbonization strategies. *Sci. Total Environ.* **2023**, *882*, 163490. [CrossRef]
70. De Masi, R.F.; Gigante, A.; Vanoli, G.P. Are nZEB design solutions environmental sustainable? Sensitive analysis for building envelope configurations and photovoltaic integration in different climates. *J. Build. Eng.* **2021**, *39*, 102292. [CrossRef]